

PRODUCTION MODEL OF TUBULAR SOLAR STILL BASED ON CONDENSATION THEORY

Teruyuki Fukuhara – fukuhara@u-fukui.ac.jp

University of Fukui, Department of Architecture & Civil Engineering

Amimul Ahasan – ahsan@members.asce.org

University Putra Malaysia, Department of Civil Engineering Faculty of Engineering

Yoshihiro Ishii – y.ishii.pu@it-hiroshima.ac.jp

Hiroshima Institute of Technology, Department of Civil Engineering & Urban Design

4. Instrumentation for renewable energy applications, www.perusolar.org

Abstract. A production model based on a film-wise condensation theory for a Tubular Solar Still taking account of the thermal resistance of the unsaturated humid air inside the still was developed in this study. The thermal resistance coefficient was reversely proportional to the dry air pressure fraction. The overall heat transfer coefficient between the humid and ambient air outside the still was used newly in the present model, because the measurement of ambient air temperature is easier than that of the inner surface temperature of the tubular cover. The analytical solution of the condensation theory could provide a good agreement with the observed production flux obtained from the laboratory experiment. Furthermore, the model prediction was compared with the field experimental data to assess the model accuracy and findings revealed that the model can be used to predict the production flux precisely.

Keywords: Condensation, Heat and mass transfer, Tubular Solar Still (TSS), Production, Unsaturated humid air

1. INTRODUCTION

Solar distillation may be one of the viable options for providing drinking water for a single house or a small community in arid or coastal regions. A basin type is the most popular among solar stills, but has the difficulty in rapid repairs and construction of the still. A new type of solar distillation, Tubular Solar Still (TSS) was designed by the authors' group to overcome the disadvantage in maintenance and management of the still. The TSS consists of a transparent tubular cover made of vinyl chloride and a trough inside the cover. Consequently, the weight of the TSS became much lighter than that of the basin type with a glass cover. The TSS, therefore, can be easily built on-site without using special tools. This easy assembly helps shortening of water transportation distance.

Many researchers (Clark, 1990, Shawaqfeh and Farid, 1995, Chaibi, 2000, Hongfei, et al., 2002) have proposed the production models of the basin type using evaporative heat and mass transfer correlations to predict distilled water output, i.e. production. The distilled water is, however, produced after the condensation which takes place on the tubular cover inner surface, following the evaporation from the water surface in a trough shown in Fig. 1. Therefore, there exists the time lag between the beginning of the production and the occurrence of the evaporation (Islam, 2006). According to the evaporation → condensation → production process in the still, it can be inferred that the theory of condensation may give a better result on the time response of the production than the past evaporation theories.

Many of condensation theories (Revenkar and Pollock, 2005, Raach and Mitrovic, 2007, Yang, et al., 2007) have been applied to a film flow achieved on a plate or a tube and derive the condensate mass flow and heat transfer rate. However, the condensation theory for a solar still has not been fully examined compared with the evaporation theories, because the data of the temperature and relative humidity of the humid air is inadequate. We recently found from our field experiments (Nagai, et al., 2002, Islam, et al., 2007) that the relative humidity of the humid air is by no means saturated (50-95%) in the daytime. From these experiments, the condensate mass transfer coefficient was obtained empirically, but the theoretical expression was not fully developed.

This paper aims to propose a production model based on a film-wise condensation theory taking account of the thermal resistance of the unsaturated humid air, and to show the validity of the proposed condensation theory by the comparison of field experimental results on the hourly production with the theoretical prediction.

2. CONDENSATION THEORY OF TSS

2.1 Energy and momentum equations

The following assumptions are made to simplify the analysis:

1. The condensate liquid film flow (hereafter liquid film flow) is a laminar flow with velocity, v_θ , and flows only along the inner circumference of the tubular cover, i.e. in the angular (θ) direction shown in Fig. 2.
2. The temperature of the liquid film surface is uniform and equal to the humid air temperature, T_{ha} . The temperature of

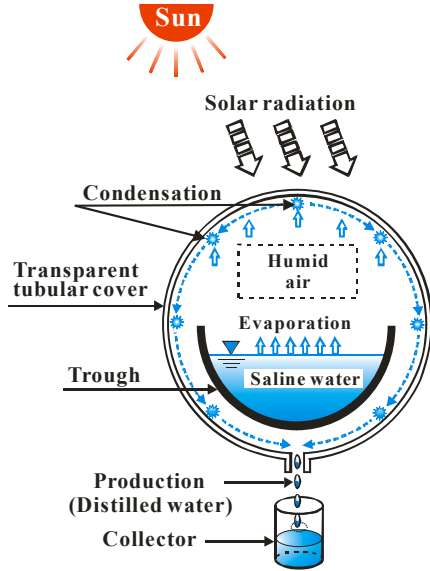


Figure 1- Production mechanism of TSS.

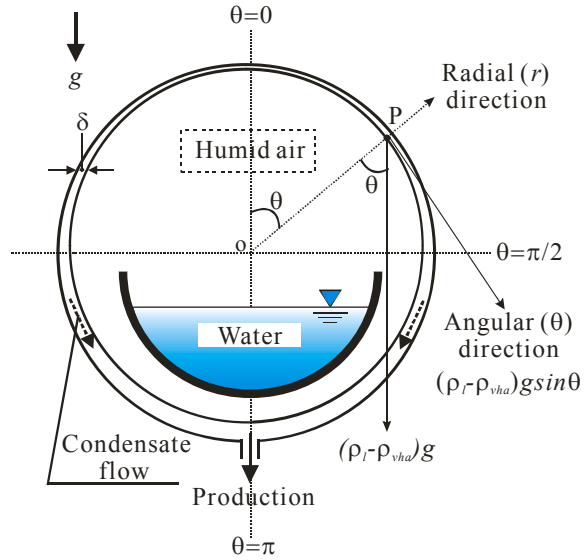


Figure 2- Liquid film flowing on inner surface of tubular cover and components of gravity force at point P.

the tubular cover, T_{ci} , is also uniform.

3. The heat transfer at the liquid film-humid air interface (interface) is caused only by condensation.
4. The temperature boundary layer exists between the humid air and the liquid film surface and the thickness, δ_{ha} , or T_{ha} may be affected by the thermal resistance associated with the presence of non-condensable gas (dry air) in the humid air (Nagai, et al., 2005).
5. The interfacial shear stress at the interface, $\tau_{i\theta}$, is negligible, i.e. $\tau_{i\theta} = 0$.
6. The gradient of v_θ in the θ direction, $dv_\theta/(rd\theta)$, is disregarded, compared with that in the radial (r) direction, $dv_\theta/(dr)$.

The governing equations of energy and momentum for the liquid film flow under thermodynamic equilibrium can be simplified, respectively, as follows:

$$\frac{d^2T}{dr^2} + \frac{1}{r} \frac{dT}{dr} = 0 \quad (1)$$

$$\left(\frac{d^2v_\theta}{dr^2} + \frac{1}{r} \frac{dv_\theta}{dr} - \frac{v_\theta}{r^2} \right) + \frac{g}{\mu_l} (\rho_l - \rho_{vha}) \sin \theta = 0 \quad (2)$$

where T is temperature of the liquid film, μ_l is the dynamic viscosity of water, ρ_l is the density of water, ρ_{vha} is the density of water vapor of the humid air and g is acceleration of gravity.

The governing equations are subjected to the following boundary conditions:

$$v_\theta = 0; T = T_{ci} \quad \text{at } r = R, 0 \leq \theta \leq \pi \quad (3)$$

$$\tau_{i\theta} = \mu_l \left[r \frac{d}{dr} \left(\frac{v_\theta}{r} \right) \right] = 0; T = T_{ha} \quad \text{at } r = R - \delta, 0 \leq \theta \leq \pi \quad (4)$$

where R is the radius of TSS and δ is the thickness of the liquid film flow.

2.2 Velocity of liquid film flow

Integrating Eq. (2) subjected to the boundary conditions of Eqs. (3) and (4), the profile of v_θ in the r direction becomes

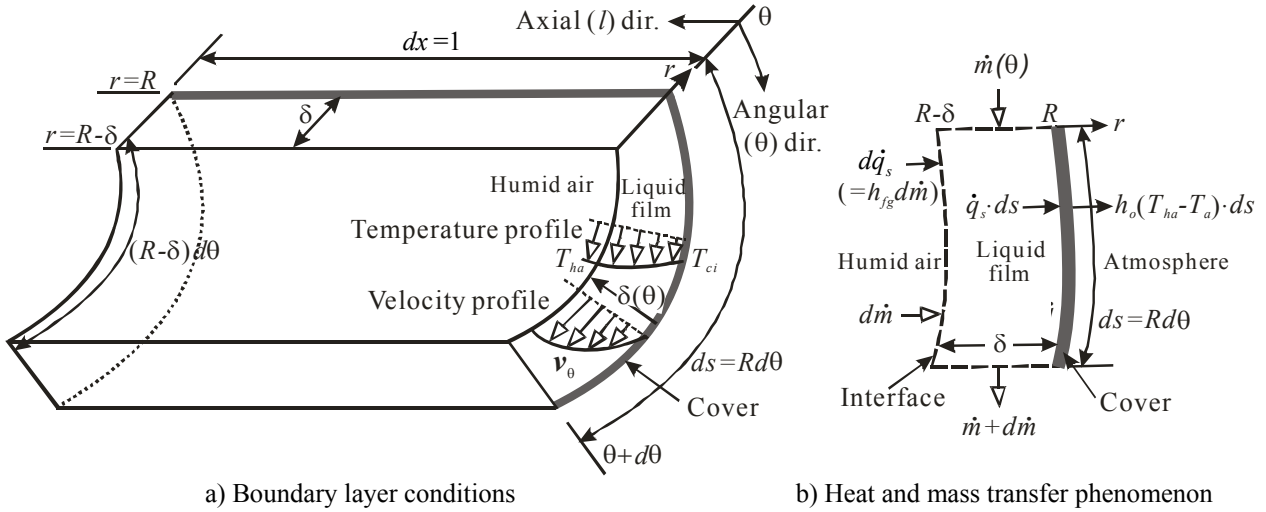


Figure 3- Boundary layer conditions and heat and mass transfer phenomenon in liquid film flow.

$$v_{\theta} = \left[\frac{S_I R}{3} + \frac{S_I (R - \delta)^3}{6R^2} \right] r - \frac{S_I (R - \delta)^3}{6r} - \frac{S_I r^2}{3} \quad (5)$$

where $S_I = \frac{g}{\mu_l} (\rho_l - \rho_{vha}) \sin \theta$.

2.3 Energy balance of liquid film flow

When the liquid film flow takes place over the whole inner area of the tubular cover, the continuity of heat flow, Q , per unit length ($dx = 1$, see Fig.3) without the thermal resistance (the assumption 4. in the section 2.1) at the interface ($r = R - \delta$) gives the following equations,

$$Q = h_i (T_{ha} - T_{ci}) dx ds' = h_{fg} d m dx = q_s dx ds' \quad (6)$$

where m is the mass flux of the liquid film flow, h_i is the heat transfer coefficient, h_{fg} is latent heat of vaporization, q_s is the conductive heat flux and ds' is the minute length in the θ direction at $r = R - \delta$.

q_s is given by Fourier's law

$$q_s = -\lambda_l \left. \frac{dT}{dr} \right|_{r=R-\delta} \quad (7)$$

where λ_l is the thermal conductivity of the condensate liquid.

Integrating Eq. (1) subjected to the boundary conditions, $T_{ci} = T|_{r=R}$ and $T_{ha} = T|_{r=R-\delta}$, the temperature gradient in Eq. (7) becomes

$$\left. \frac{dT}{dr} \right|_{r=R-\delta} = - \frac{T_{ha} - T_{ci}}{(R - \delta) \ln \left(\frac{R - \delta}{R} \right)} \quad (8)$$

Since δ is fairly small compared to R , Eq. (8) is approximated as

$$\left. \frac{dT}{dr} \right|_{r=R-\delta} \approx - \frac{T_{ha} - T_{ci}}{\delta(\theta)} \quad (9)$$

Inserting Eq. (9) into Eq. (7) yields

$$q_s = \frac{\lambda_l (T_{ha} - T_{ci})}{\delta} \quad (10)$$

Taking account of the fact that the liquid film flow takes place locally (the liquid film flow does not appear uniformly in the longitudinal (x) direction) and of the thermal resistance, Q and q_s may be transformed as \dot{Q} and \dot{q}_s , respectively:

$$\dot{Q} = \dot{h}_l (T_{ha} - T_{ci}) dx ds' = h_{fg} \dot{m} dx = \dot{q}_s dx ds' = -\gamma_1 \gamma_2 \lambda_l \left. \frac{dT}{dr} \right|_{r=R} dx ds' \quad (11)$$

$$\dot{q}_s = \gamma_c \lambda_l \frac{(T_{ha} - T_{ci})}{\delta} \quad (12)$$

where \dot{m} is the mass flux of the local liquid film flow and \dot{Q} is the net heat per the minute area ($ds' dx (=1)$). \dot{h}_l and \dot{q}_s are the heat transfer coefficient and heat flux associated with the thermal resistance and local liquid film flow due to nonuniform condensation, respectively. γ_1 is the correction coefficient of the temperature gradient in Eq. (11). γ_2 means the ratio of the area of the local liquid film flow to the whole inner surface area of the tubular cover. The value of γ_1 may depend on dry air pressure fraction (Nagai, et al., 2005). If the thermal resistance is ignored, γ_1 becomes 1. When $\gamma_1 \gamma_2$ is replaced as the total thermal efficiency coefficient, γ_c , \dot{h}_l is described as the following equation by using Eqs. (11) and (12):

$$\dot{h}_l = \gamma_c \frac{\lambda_l}{\delta} \quad (13)$$

Comparing a set of Eqs. (6) and (7) with a set of Eqs. (11) and (12), the following relation is found:

$$\frac{\dot{h}_l}{h_l} = \frac{\dot{q}_s}{q_s} = \frac{d\dot{m}}{dm} = \gamma_c \quad (14)$$

\dot{m} , therefore, can be obtained by the following integration:

$$\dot{m} = \gamma_c \int_{R-\delta}^R \rho_l v_\theta dr \quad (15)$$

Substituting Eq. (5) into Eq. (15) yields

$$\dot{m} = \gamma_c \frac{\rho_l S_l \delta^3}{3} = \gamma_c \frac{g \rho_l (\rho_l - \rho_{vha}) \delta^3 \sin \theta}{3 \mu_l} \quad (16)$$

By using the relation, $ds = R d\theta$, and Eq. (16), \dot{q}_s is written as

$$\dot{q}_s = h_{fg} \frac{d\dot{m}}{R d\theta} = h_{fg} \frac{d\dot{m}}{d\delta} \frac{d\delta}{R d\theta} \quad (17)$$

Differentiating Eq. (16) in terms of δ yields

$$\frac{d\dot{m}}{d\delta} = \gamma_c \frac{g \rho_l (\rho_l - \rho_{vha}) \delta^2 \sin \theta}{\mu_l} \quad (18)$$

Substituting Eqs. (12) and (18) into Eq. (17), the following relation is derived:

$$\delta^3 d\delta = \frac{\lambda_l \mu_l D (T_{ha} - T_{ci})}{2 g \rho_l (\rho_l - \rho_{vha}) h_{fg}} \frac{d\theta}{\sin \theta} = A \frac{d\theta}{\sin \theta} \quad (19)$$

where $A = \frac{\lambda_l \mu_l D (T_{ha} - T_{ci})}{2g\rho_l(\rho_l - \rho_{vha})h_{fg}}$, in which $D (=2R)$ is the diameter of TSS.

Integrating Eq. (19) subjected to the boundary condition, $\delta = 0$ at top of the tubular cover, i.e. $\theta = \theta_0 (\approx 0)$, yields the variation of δ in the θ direction,

$$\delta = \left[4A \ln \left| \tan \frac{\theta}{2} / \tan \frac{\theta_0}{2} \right| \right]^{1/4} \quad (20)$$

2.4 Heat transfer coefficient of unsaturated humid air

Substituting Eq. (20) into Eq. (13), \dot{h}_l is given by

$$\dot{h}_l = \gamma_c \lambda_l \left[4A \ln \left| \tan \frac{\theta}{2} / \tan \frac{\theta_0}{2} \right| \right]^{-1/4} \quad (21)$$

The average heat transfer coefficient of the liquid film, h_c , is given by the following integration in terms of θ .

$$h_c = \frac{1}{(\theta_l - \theta_o)} \int_{\theta_o}^{\theta_l} \dot{h}_l d\theta \quad (22)$$

Since $\theta_o = 0^\circ$ cannot be applied to the integration of Eq. (22), $\theta_o = 1^\circ$ is chosen and $\theta_l = 180^\circ$ is given in this paper.

$$h_c = 0.996 \gamma_c \left[\frac{g\rho_l(\rho_l - \rho_{vha})h_{fg}\lambda_l^3}{\mu_l D (T_{ha} - T_{ci})} \right]^{1/4} \quad (23)$$

Eq. (6) is, however, not practical, because the measurement (and accuracy) of T_{ci} is not easy (and low), compared to those of T_w , T_{ha} and T_a . We propose, therefore, a new overall heat transfer coefficient, h_o , defined by the following equation:

$$h_o (T_{ha} - T_a) = h_c (T_{ha} - T_{ci}) \quad (24)$$

Eq. (24) allows the calculation of \dot{q}_s as the product of h_o and the difference in temperature between the inside and outside of a TSS, i.e. $T_{ha} - T_a$. Supposing that the temperature difference fraction, $a = (T_{ha} - T_{ci}) / (T_{ha} - T_a)$, is constant, h_o is expressed as

$$h_o = 0.996 \gamma_c \left[\frac{g\rho_l(\rho_l - \rho_{vha})h_{fg}a^3\lambda_l^3}{\mu_l D (T_{ha} - T_a)} \right]^{1/4} \quad (25)$$

Thus, \dot{m} is calculated by

$$\dot{m} = h_o (T_{ha} - T_a) / h_{fg} \quad (26)$$

Substituting Eq. (25) into Eq. (26), γ_c is calculated by the following equation:

$$\gamma_c = \frac{\dot{m}}{0.996} \left[\frac{\mu_l D h_{fg}^3}{g\rho_l(\rho_l - \rho_{vha})a^3\lambda_l^3 (T_{ha} - T_a)^3} \right]^{1/4} \quad (27)$$

3. EXPERIMENTAL METHOD AND CONDITIONS

3.1 Laboratory experiments (Islam, 2006)

To find the properties of γ_c and a , our laboratory experimental results were quoted in this paper. Laboratory

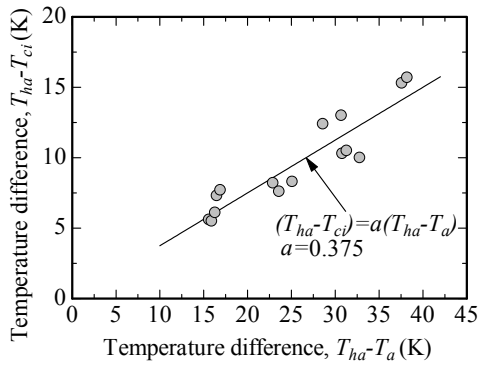


Figure 4- Relation between temperature difference ($T_{ha} - T_{ci}$) and temperature difference ($T_{ha} - T_a$).

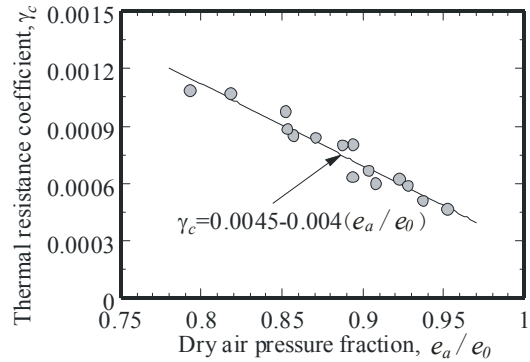


Figure 5- Relation between thermal resistance coefficient, γ_c , and dry air pressure fraction, e_a/e_0 .

Table 1. Laboratory experimental conditions and observed steady state values.

| Case No. | Experimental conditions | | | Observed values | |
|----------|---------------------------|------------|------------|-----------------|---------------|
| | R_s (W/m ²) | T_a (°C) | RH_a (%) | T_{ha} (°C) | RH_{ha} (%) |
| 1 | | 35.3 | | 66.1 | 78 |
| 2 | | 32.1 | | 63.4 | 78 |
| 3 | 1200 | 26.6 | 35 | 59.4 | 77 |
| 4 | | 22.2 | | 59.8 | 73 |
| 5 | | 17.0 | | 55.2 | 72 |
| 6 | | 35.3 | | 58.2 | 81 |
| 7 | | 32.0 | | 55.6 | 81 |
| 8 | 800 | 26.5 | 35 | 51.6 | 81 |
| 9 | | 22.4 | | 51.0 | 76 |
| 10 | | 16.2 | | 46.9 | 75 |
| 11 | | 35.1 | | 50.7 | 85 |
| 12 | | 31.7 | | 47.6 | 86 |
| 13 | 500 | 26.5 | 35 | 42.8 | 86 |
| 14 | | 22.7 | | 39.2 | 90 |
| 15 | | 17.0 | | 33.9 | 90 |

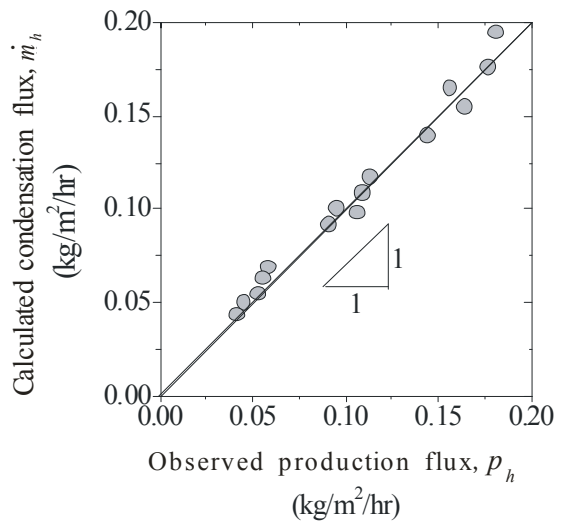


Figure 6- Comparison of calculated hourly condensation flux, \dot{m}_h , with observed hourly production flux, p_h .

experiments on the productivity of a TSS were conducted in a thermostatic room to keep a constant ambient air temperature and relative humidity. The equipment consisted of a TSS, a solar simulator, two electric balances, a data logger and two computers. The TSS was comprised with a tubular cover and a semicircular black trough in it. The tubular cover used in the experiment was made of a curled transparent vinyl chloride sheet of 0.5mm in thickness. The length and outside diameter were 0.52m and 0.13m, respectively. The trough was made of vinyl chloride with 10mm in thickness, 0.1m in outside diameter and 0.49m in length. Production was enhanced with 12 infrared lamps (125W) and the radiant heat flux, R_s , was controlled by changing the height of the lamps. The temperatures (T_{ha} , T_{ci} and T_a), RH_{ha} and R_s were measured by thermo-couples, a thermo-hygrometer and a pyranometer, respectively. All data were automatically recorded into the data logger and computers at one-minute interval.

Tab. 1 shows the experimental conditions. The production was measured under the three different levels of R_s and five different T_a , respectively.

3.2 Field experiments (Islam, 2007)

Our field experimental results were also quoted to support the validity of the condensation theory. The same specification of TSS was fabricated for the filed experiments.

4. RESULTS AND DISCUSSIONS

4.1 Laboratory experiments

Fig. 4 shows the relation between ($T_{ha} - T_{ci}$) and ($T_{ha} - T_a$). It is seen from the straight regression line that the temperature difference fraction, a , is 0.375. Since the condensation rate was not measured, γ_c was calculated by Eq. (27) under the assumption that the condensation flux is equal to the production flux.

Nagai et al. (2005) pointed out that the total thermal resistance between humid air and vertical cooled surface

decreases as the relative humidity of humid air increases. According to this idea, we suppose that γ_c is expressed by the dry air pressure fraction, e_a/e_o (= partial dry air pressure/total atmospheric pressure).

Fig. 5 shows the relation between γ_c and e_a/e_o . The value of γ_c is reversely proportional to e_a/e_o and the regression can be given by the following equation:

$$\gamma_c = 0.0045 - 0.004 \frac{e_a}{e_o} \quad (28)$$

where $\frac{e_a}{e_o} = 1 - \frac{e_{vha}}{e_o}$; $e_{vha} = f(T_{ha}, RH_{ha})$.

Substituting Eq. (28) and $a = 0.375$ into Eq. (25), h_o is expressed by

$$h_o = \left(2.15 - 1.91 \frac{e_a}{e_o} \right) \left[\frac{g\rho_l(\rho_l - \rho_{vha})h_{fg}\lambda_l^3}{\mu_l D(T_{ha} - T_a)} \right]^{\frac{1}{4}} \times 10^{-3} \quad (29)$$

The hourly condensation mass flux, \dot{m}_h , is expressed as

$$\dot{m}_h = \frac{3600h_o(T_{ha} - T_a)}{h_{fg}} \quad (30)$$

Fig. 6 shows the comparison of \dot{m}_h calculated by Eq. (30) with the observed hourly production flux, p_h . Eq. (30) provides a good agreement with the observed hourly production flux, p_h .

4.2 Field experiments

Fig. 7 shows the observed diurnal variations of T_{ha} , T_a and RH_{ha} obtained in Fukui, Japan on September 29 and October 6, 2005. T_{ha} rose rapidly after sunrise (approximately 6:00) and peaked between 12:00 to 13:00 for both days. RH_{ha} was remarkably below 100% in the daytime (minimum 50%) but about 100% during the night.

Fig. 8 shows the diurnal variations of p_h obtained from the field experiment and \dot{m}_h calculated by Eq. (30). The profile of p_h is almost the same as that of \dot{m}_h and a time lag between the condensation and the production can be negligible as far as the TSS used in the experiment is concerned.

Fig. 9 shows the comparison between p_h and \dot{m}_h . Both agree well with each other. From Figs. 8 and 9, it is known that p_h is allowed to be replaced with \dot{m}_h .

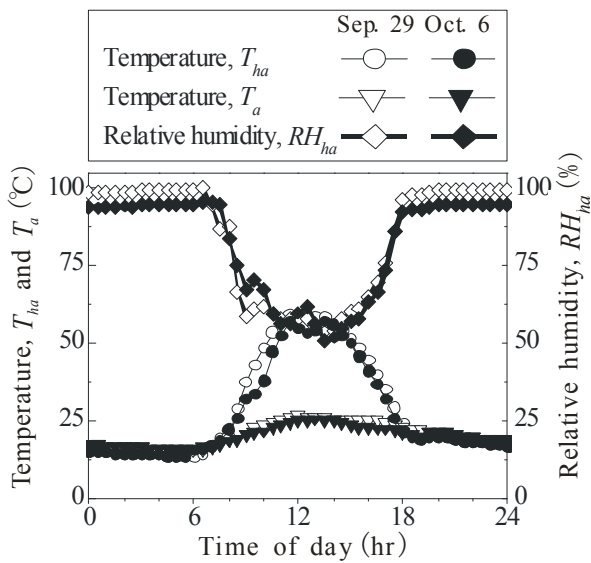


Figure 7- Diurnal variations of temperatures and relative humidity obtained on September 29 and October 6, 2005 in Fukui, Japan.

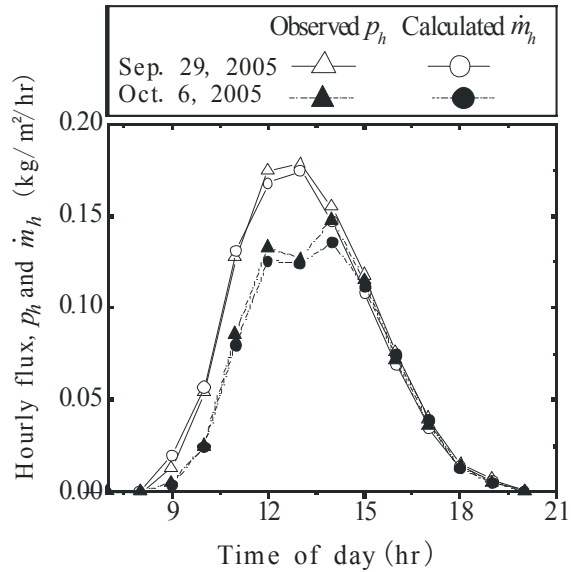


Figure 8- Diurnal variations of observed hourly production flux, p_h , and calculated hourly condensation flux, \dot{m}_h .

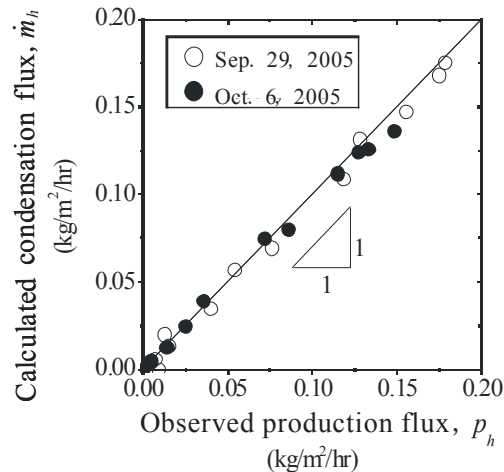


Figure 9- Comparison of calculated hourly condensation flux, \dot{m}_h , with observed hourly production flux, p_h .

5. CONCLUSIONS

A production model based on the condensation theory of a Tubular Solar Still taking account of the thermal resistance of the unsaturated humid air and nonuniform condensate liquid film flow is presented in this paper. It was revealed that the thermal resistance coefficient was in reverse proportion to the dry air pressure fraction. The present condensation theory using the overall heat transfer coefficient between the humid and ambient air could provide a good agreement with the hourly production flux obtained from the laboratory experiment. Moreover, the validity of the condensation theory was evaluated from the comparison with the field experimental data and it is concluded that the present condensation theory can be used to predict the production flux precisely.

REFERENCES

- Chaibi, M. T. 2000. Analysis by simulation of a solar still integrated in a greenhouse roof, *Desalination*, vol. 128, pp. 123-138.
- Clark, J. A. 1990. The steady-state performance of a solar still, *Solar Energy*, vol. 44, n. 1, pp. 43-49.
- Hongfei, Z., Xiaoyan, Z., Jing, Z. and Yuyuan, W. 2002. A group of improved heat and mass transfer correlations in solar stills, *Energy Conservation & Management*, vol. 43, pp. 2469-2478.
- Islam, K. M. S. 2006. Heat and Vapor Transfer in Tubular Solar Still and Its Production Performance, Doctoral thesis, Department of Architecture & Civil Engineering, University of Fukui, Japan, pp. 33-52.
- Islam, K. M. S., Fukuhara, T. and Ahsan, A. 2007. Tubular solar still-an alternative small scale fresh water management, *Proc. Int. Conf. Water and Flood Management (ICWFM-2007)*, Bangladesh, pp. 291-298.
- Nagai, N., Takeuchi, M., Masuda, S., Yamagata, J., Fukuhara, T. and Takano, Y. 2002. Heat transfer modeling and field test on basin-type solar distillation device, *Proc. IDA World Cong.*, Bahrain, CD-ROM, BAH03-072.
- Nagai, N., Kura, O., Takeuchi, M. and Masuda, T. 2005. Experimental study on free-convection condensation heat transfer from moist air, *Proc. 2005 ASME Summer Heat Transactional Conference, USA*, CD-ROM, HT2005-72608.
- Raach, H. and Mitrovic, J. 2007. Simulation of heat and mass transfer in a multi-effect distillation plant for sea water desalination, *Desalination*, vol. 204, pp. 416-422.
- Revankar, S. T. and Pollock, D. 2005. Laminar film condensation in a vertical tube in the presence of noncondensable gas, *Applied Mathematical Modeling*, vol. 29, pp. 341-359.
- Shawaqfeh, A. T. and Farid, M. M. 1995. New development in the theory of heat and mass transfer in solar stills, *Solar Energy*, vol. 55 (6), pp. 527-535.
- Yang, S. A., Li, G. C. and Yang, W. J. 2007. Thermodynamic optimization of free convective film condensation on a horizontal elliptical tube with variable wall temperature, *Int. J. Heat & Mass Transfer*, vol. 50 (23-24), pp. 4607-4613.